



# Chemical generation of small molecule-based bispecific antibody-drug conjugates for broadening the target scope

Aiko Yamaguchi<sup>a</sup>, Yasuaki Anami<sup>a</sup>, Summer Y.Y. Ha<sup>a</sup>, Travis J. Roeder<sup>a</sup>, Wei Xiong<sup>a</sup>, Jangsoon Lee<sup>b</sup>, Naoto T. Ueno<sup>b</sup>, Ningyan Zhang<sup>a</sup>, Zhiqiang An<sup>a</sup>, Kyoji Tsuchikama<sup>a,\*</sup>

<sup>a</sup> Texas Therapeutics Institute, The Brown Foundation Institute of Molecular Medicine, The University of Texas Health Science Center at Houston, Houston, TX, USA

<sup>b</sup> Section of Translational Breast Cancer Research, Department of Breast Medical Oncology, The University of Texas MD Anderson Cancer Center, Houston, TX, USA

## ARTICLE INFO

### Keywords:

Antibody drug conjugate  
Bispecific  
Conjugation  
Breast cancer  
Cancer  
Chemotherapy  
Heterogeneity  
Linker

## ABSTRACT

Antibody-drug conjugates (ADCs) hold great therapeutic promise for cancer indications; however, treating tumors with intratumor heterogeneity remains challenging. We hypothesized that ADCs that can simultaneously target two different cancer antigens could address this issue. Here, we report controlled production and evaluation of bispecific ADCs chemically functionalized with tumor-targeting small molecules. Enzyme-mediated conjugation of bi-functional branched linkers and following sequential orthogonal click reactions with payload and tumor targeting modules (folic acid or RGD peptide) afforded homogeneous bispecific ADCs with defined ligand/drug-to-antibody ratios ranging from 4 + 4 to 16 + 4 (ligand/payload). Most bispecific ADCs were stable under physiological conditions for 14 days. Functionalization with the cancer-specific ligands did not impair cathepsin B-mediated payload release from ADCs. Bispecific ADCs targeting the folate receptor (FR)/human epidermal growth factor receptor 2 (HER2) demonstrated specific binding and high cell killing potency only in cells expressing either antigen (FR or HER2). Integrin/HER2 bispecific ADCs equipped with RGD peptides also showed target-specific binding and cytotoxicity in integrin- or HER2-positive cells. These findings suggest that our small-molecule based bispecific ADCs have the potential to effectively treat tumors with heterogeneous antigen expression.

## 1. Introduction

Antibody-drug conjugates (ADCs) hold great therapeutic promise for cancer indications.<sup>1–4</sup> The clinical potential of ADCs has been stimulating research and investment interests, as seen for nine FDA-approved ADCs and >100 ADCs in clinical trials (clinicaltrials.gov). Most ADCs require binding to their antigen and following internalization to release payloads and exert cytotoxicity against target cells. As such, treating tumors with intratumor heterogeneity remains a challenge in ADC-based cancer therapy. Indeed, intratumor HER2 heterogeneity makes trastuzumab emtansine (Kadcyla® or known as T-DM1), a FDA-approved ADC, less effective for treating breast tumors expressing relatively low levels of HER2.<sup>5</sup> Hydrophobic ADC payloads can eradicate neighboring antigen-negative cells upon release from the initially

targeted cell (bystander effect). However, tumor cells expressing multi drug resistance pumps (e.g., P-glycoprotein) are often insensitive against such hydrophobic payloads. Therefore, broadening the target scope and improving ADC delivery efficiency could help overcome intratumor heterogeneity and further increase the clinical potential of ADCs.

The use of bispecific antibodies that can simultaneously target two different tumor antigens is a promising approach to expanding the target scope of ADCs.<sup>6</sup> Bispecific antibody is a general term for a variety of dual-targeting antibodies such as relatively small proteins consisting of two linked antigen-binding fragments and large immunoglobulin G (IgG)-like molecules with additional antigen-binding fragments attached. Traditional bispecific ADCs consisting of two distinct Fab arms have shown certain treatment efficacy for tumors with intratumor heterogeneity.<sup>7–12</sup> However, loss of the bivalent binding modality to each

**Abbreviations:** ADC, antibody-drug conjugate; DBCO, dibenzocyclooctyne; FA, folic acid; FRA, folate receptor a; HER2, human epidermal growth factor receptor 2; HIC, hydrophobic interaction chromatography; IgG, immunoglobulin G; MMAF, monomethyl auristatin F; PABC, *p*-aminobenzyloxycarbonyl; PEG, polyethylene glycol; RGD, Arg-Gly-Asp; SEC, size-exclusion chromatography; TCO, *trans*-cyclooctene.

\* Corresponding author at: Texas Therapeutics Institute, The Brown Foundation Institute of Molecular Medicine, The University of Texas Health Science Center at Houston, 1881 East Road, Houston, TX 77054, USA.

E-mail address: [Kyoji.Tsuchikama@uth.tmc.edu](mailto:Kyoji.Tsuchikama@uth.tmc.edu) (K. Tsuchikama).

<https://doi.org/10.1016/j.bmc.2021.116013>

Received 17 November 2020; Received in revised form 31 December 2020; Accepted 4 January 2021

Available online 9 January 2021

0968-0896/© 2021 Elsevier Ltd. All rights reserved.

antigen could lead to suboptimal antigen binding and internalization.<sup>7–10</sup> Another intriguing form is antibodies functionalized with tumor-targeting small molecules.<sup>13–16</sup> In contrast to traditional bispecific ADCs, small molecule-based bispecific ADCs harbor two identical Fab arms, which in theory retain optimal antigen binding and internalization profiles. The number of small molecules incorporated into the ADC scaffold and the conjugation sites can significantly affect ADC physicochemical properties and antigen binding.<sup>17</sup> Considering two components (i.e., payload and cancer-targeting small molecules) need to be installed simultaneously, the conjugation format plays a critical role in the generation of small molecule-based bispecific ADCs.

We have recently developed click chemistry-based branched linkers that can site-specifically incorporate two distinct payload molecules onto a single antibody.<sup>18</sup> This technology enables flexible production of a variety of dual-drug ADCs with controlled drug-to-antibody ratios (DARs) ranging from 2 + 2 to 4 + 2. Based on this finding, we envisioned that our branched linker technologies could be used to generate novel small molecule-based bispecific ADCs with high homogeneity and unique targeting profiles. Herein, we report a chemical method for constructing bispecific ADCs using our branched linkers and their potential for eradicating a broad range of tumor cells. We selected folic acid (FA) and arginylglycylaspartic acid (Arg-Gly-Asp or RGD) as models of tumor-specific ligands. These are representative, clinically validated small molecules for active tumor targeting and drug delivery. A variety of cancer cells overexpress the folate receptor (FR) that strongly interacts with and internalizes FA ( $K_D = 0.1–1$  nM).<sup>15,19</sup> Cyclic RGD peptides bind preferentially to the  $\alpha\beta_3$  integrin, a receptor that plays roles in angiogenesis and is expressed in tumor endothelial cells as well as on some tumor cells.<sup>20,21</sup>

## 2. Results and discussion

### 2.1. Design and preparation of homogeneous folate receptor (FR)/HER2 bispecific ADCs

Based on the linker technologies reported by our group,<sup>22,23</sup> we have

developed branched ADC linkers that enable site-specific and quantitative installation of two distinct payload molecules onto a single antibody through sequential orthogonal strain-promoted azide–dibenzocyclooctyne (DBCO) cycloaddition and methyltetrazine–*trans*-cyclooctene (TCO) cycloaddition.<sup>18</sup> To construct FR/HER2 bispecific ADCs using this technology, we designed FA modules consisting of TCO as a click handle, polyethylene glycol (PEG) spacer ( $n = 4$  or 24), and FA (Figure 1). FA has two carboxyl groups at the alpha ( $\alpha$ ) and gamma ( $\gamma$ ) positions of its glutamate moiety, which are available for derivatization. To evaluate how the derivatization position and the degree of exposure of the FA moiety affect the biological behavior of bispecific ADCs, we designed and synthesized three TCO-FA modules: TCO-peg4- $\alpha$ - or  $\gamma$ -conjugated FA and TCO-peg24-mixed FA (a mixture of  $\alpha$ - and  $\gamma$ -regioisomers). For payload installation, we used a payload module consisting of DBCO as a click reaction handle, PEG spacer, glutamic acid–valine–citrulline (GluValCit) cleavable linker, *p*-aminobenzoyloxycarbonyl (PABC) group for traceless payload release, and monomethyl auristatin F (MMAF) as a payload.<sup>24</sup> We have shown that the GluValCit linker system ensures ADC *in vivo* efficacy while minimizing premature linker degradation in human and mouse plasma.<sup>22,23,25</sup> Microbial transglutaminase (MTGase)-mediated transpeptidation exclusively connected the bi-functional di-arm linker to the side chain of glutamine 295 (Q295) and 297 (Q297) within a N297Q anti-HER2 mAb to afford a highly homogeneous antibody–linker conjugate (first and second panels, Figure 2A). Subsequently, the anti-HER2 mAb–di-arm linker conjugate underwent consecutive methyltetrazine–TCO and azide–DBCO cycloadditions in one pot with TCO-peg4- $\alpha$ -conjugated FA and DBCO–MMAF modules. These cycloadditions provided a FR/HER2 bispecific ADC with a ligand/drug to antibody ratio (L/DAR) of 4 + 4 (FA/MMAF) in a quantitative and selective manner (third and fourth panels, Figure 2A). Highly homogeneous FR/HER2 bispecific ADCs equipped with TCO-peg4- $\gamma$ -conjugated FA or TCO-peg24-mixed FA were prepared in a similar manner (Figure 2B). As shown in the LC-MS traces, this sequential conversion exclusively yielded desired conjugates without cross reactions between mismatched click pairs. To demonstrate that this methodology is broadly applicable,

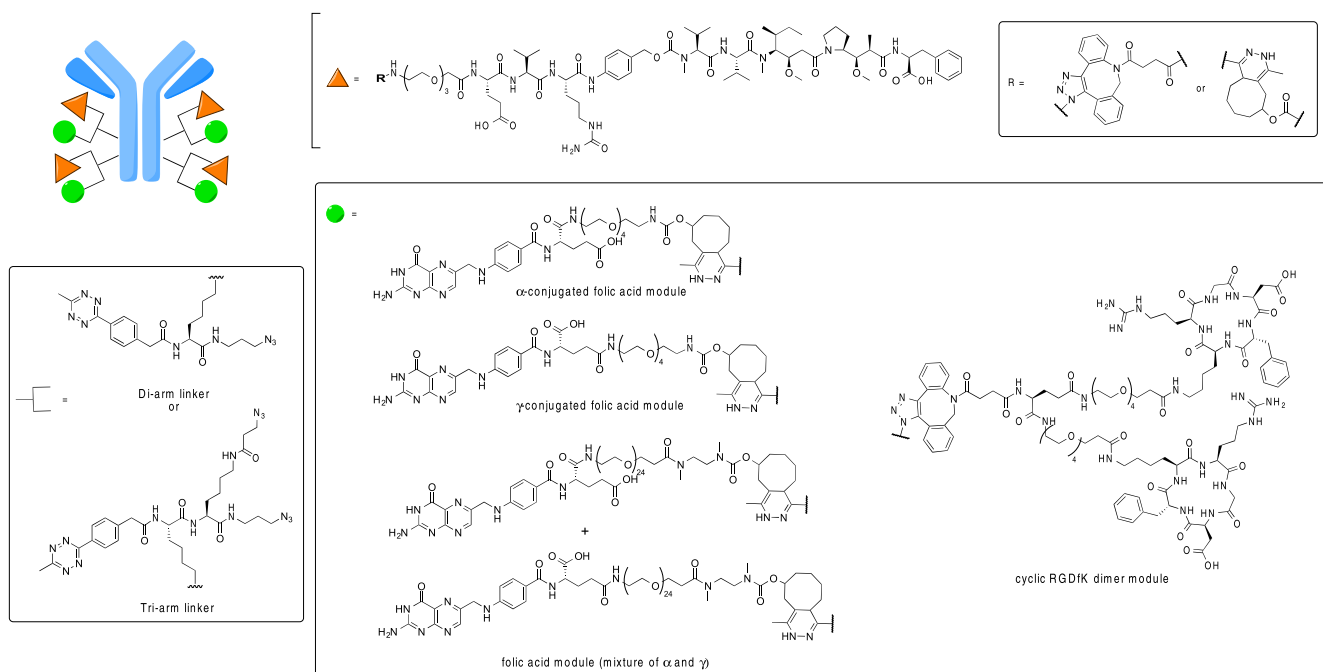


**Figure 1.** Molecular design of small-molecule based bispecific ADCs. MTGase-mediated conjugation of bi-functional branched linkers and following sequential orthogonal click reactions with payloads and tumor-targeting modules (FA or RGD) afford homogeneous bispecific ADCs with defined L/DARs (light green circle: FA or RGD molecule; orange triangle: MMAF). MTGase, microbial transglutaminase; L/DAR, ligand/drug-to-antibody ratio; MMAF, monomethyl auristatin F.

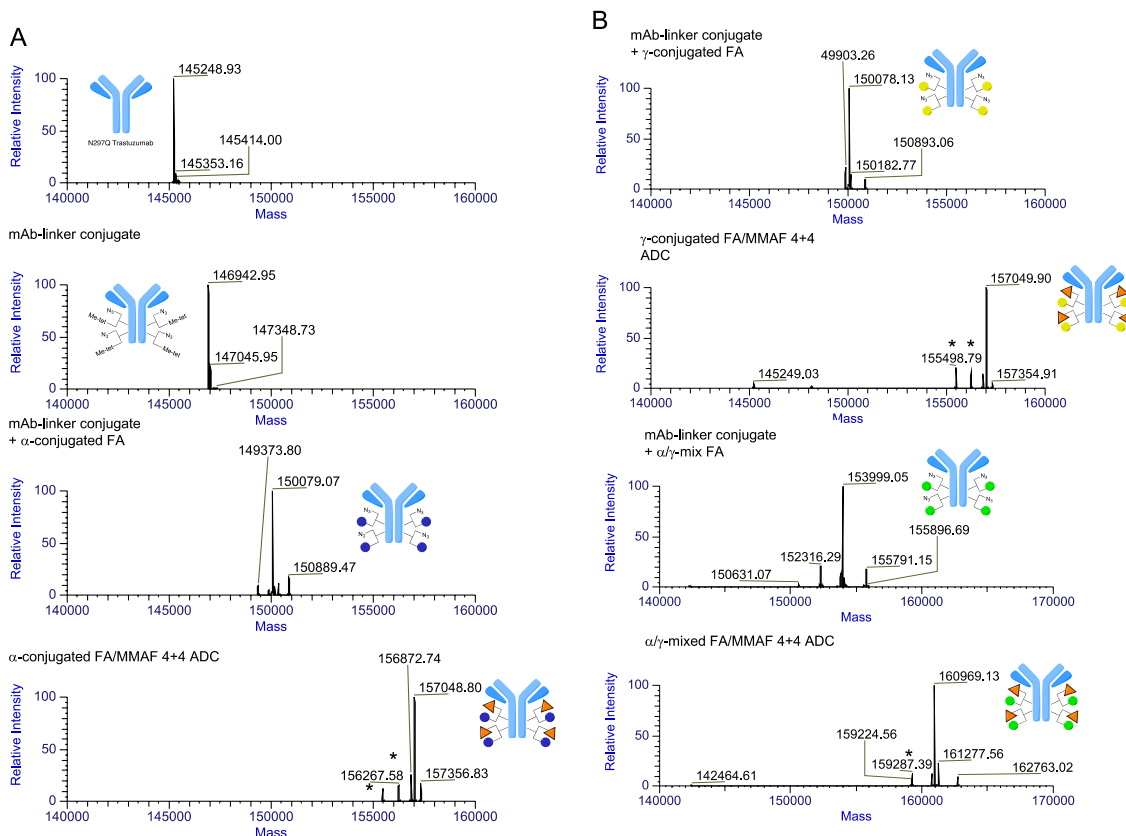


**Figure 2.** Construction of FR/HER2 bispecific ADCs. A, B: Deconvoluted ESI-mass spectra. A, First panel: intact N297Q anti-HER2 mAb (trastuzumab mutant). Second panel: mAb-branched linker conjugate. Third panel: intermediate after conjugation with TCO- $\alpha$ -conjugated FA modules (blue circle). Fourth panel: highly homogeneous FR/HER2 bispecific ADCs with a L/DAR of 4 + 4 ( $\alpha$ -conjugated FA + MMAF, depicted as an orange triangle). Asterisk (\*) indicates fragment ions detected in ESI-MS analysis. B, first and third panel: intermediate after conjugation with TCO- $\gamma$ -conjugated or mixed FA modules (yellow and green circles, respectively). Fourth panel: highly homogeneous FR/HER2 bispecific ADCs with a L/DAR of 4 + 4 ( $\gamma$ -conjugated or mixed FA + MMAF).

we performed the same conjugation with a N297Q anti-epidermal growth factor receptor (EGFR) mAb. We could successfully obtain anti-FR/EGFR ADCs with high homogeneity (Figure S1).

## 2.2. Characterization of FR/HER2 bispecific ADCs

To assess the relative hydrophobicity of the bispecific ADCs, we performed hydrophobic interaction chromatography (HIC) analysis under physiological conditions (phosphate buffer, pH 7.4). All

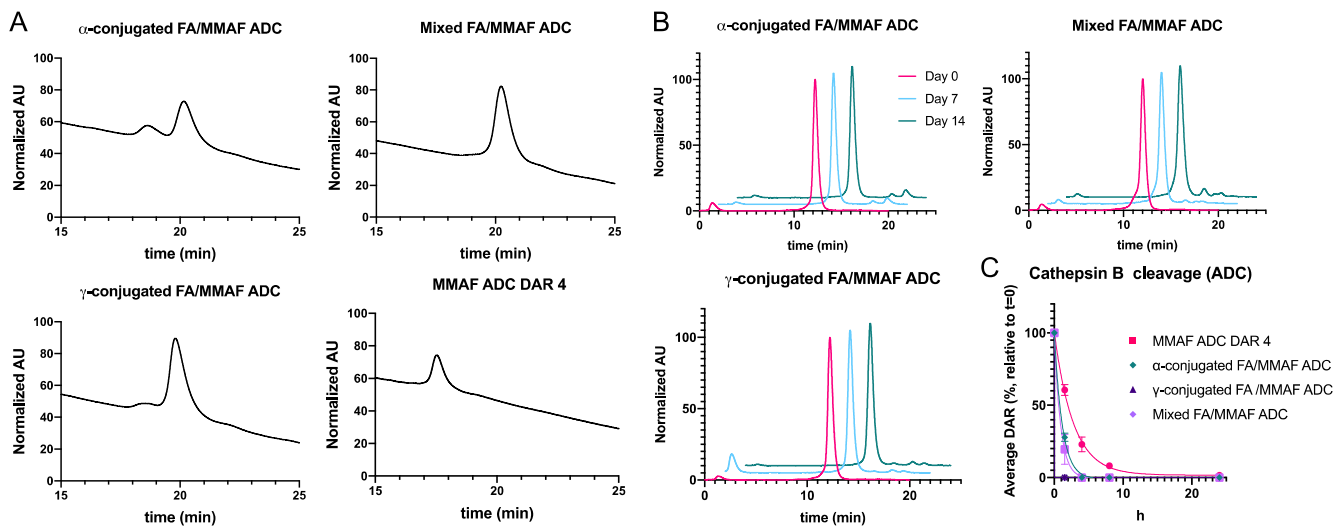


**Figure 3.** Characterization of FR/HER2 bispecific ADCs. A, Hydrophobic interaction chromatography (HIC) analysis of ADCs under physiological conditions (phosphate buffer, pH 7.4). B, Overlay traces of size-exclusion chromatography (SEC) after incubating each conjugate in PBS (pH 7.4) at 37 °C for 0–14 days. C, Human cathepsin B mediated cleavage of ADCs at 37 °C. The degree of loss of payload in each ADC was determined by LCMS. All assays were performed more than twice in technical duplicate. Error bars represent s.e.m. (n = 2).

conjugates showed comparable hydrophobicity (Figure 3A). Despite the high loading rate (L/DAR 4 + 4), no conjugates showed significant increase in retention time (>5 min) compared to a MMAF ADC with a DAR of 4. This is likely owing to relatively high hydrophilicity of the FA modules. Next, we assessed the FR/HER2 bispecific ADCs for in vitro stability. Size-exclusion chromatography (SEC) analysis revealed that >94% of the FR/HER2 bispecific ADCs remained intact after incubation in phosphate-buffered saline (PBS) at 37 °C for 14 days (Figure 3B). Then, we evaluated the FR/HER2 bispecific ADCs for payload release upon cathepsin B-mediated cleavage (Figure 3C). When our FR/HER2 bispecific ADCs were incubated with human liver cathepsin B at 37 °C, payloads were completely released from all ADCs tested within 4 h. It took up to 24 h for the complete release of MMAF from an anti-HER2 monospecific ADC (DAR 4). Although an in-depth mechanistic study is needed for clarification, these results indicate that the FA/payload dual conjugation promotes rather than impairs cathepsin B-mediated cleavage of the GluValCit-PABC sequence within each payload module.

Overall, these findings suggest that our molecular design does not compromise ADC physicochemical properties.

### 2.3. Binding of bispecific FR/HER2 ADCs to FR- and/or HER2-positive cells

To test the bispecific FR/HER2 ADCs for binding affinity for FR and HER2, we performed cell-based enzyme-linked immunosorbent assay (ELISA). The human cell lines KB (FR-positive, HER2-negative), KPL-4 (FR-negative, HER2-positive), and human embryonic kidney 293 (HEK293; FR- and HER2-negative) were used (Figure 4A). The  $\alpha$ ,  $\gamma$ -mixed FA-conjugated bispecific FR/HER2 ADC showed high binding affinity for FR-positive, HER2-negative KB cells, while the parent anti-HER2 mAb did not. Binding of  $\alpha$ - or  $\gamma$ -conjugated FA-modified bispecific FR/HER2 ADCs to KB cells was modest. This result suggests that the difference in the PEG linker length ( $n = 4$  for  $\alpha$ - or  $\gamma$ -conjugated FA modules and  $n = 24$  for  $\alpha$ ,  $\gamma$ -mixed FA modules) could impact how the FA

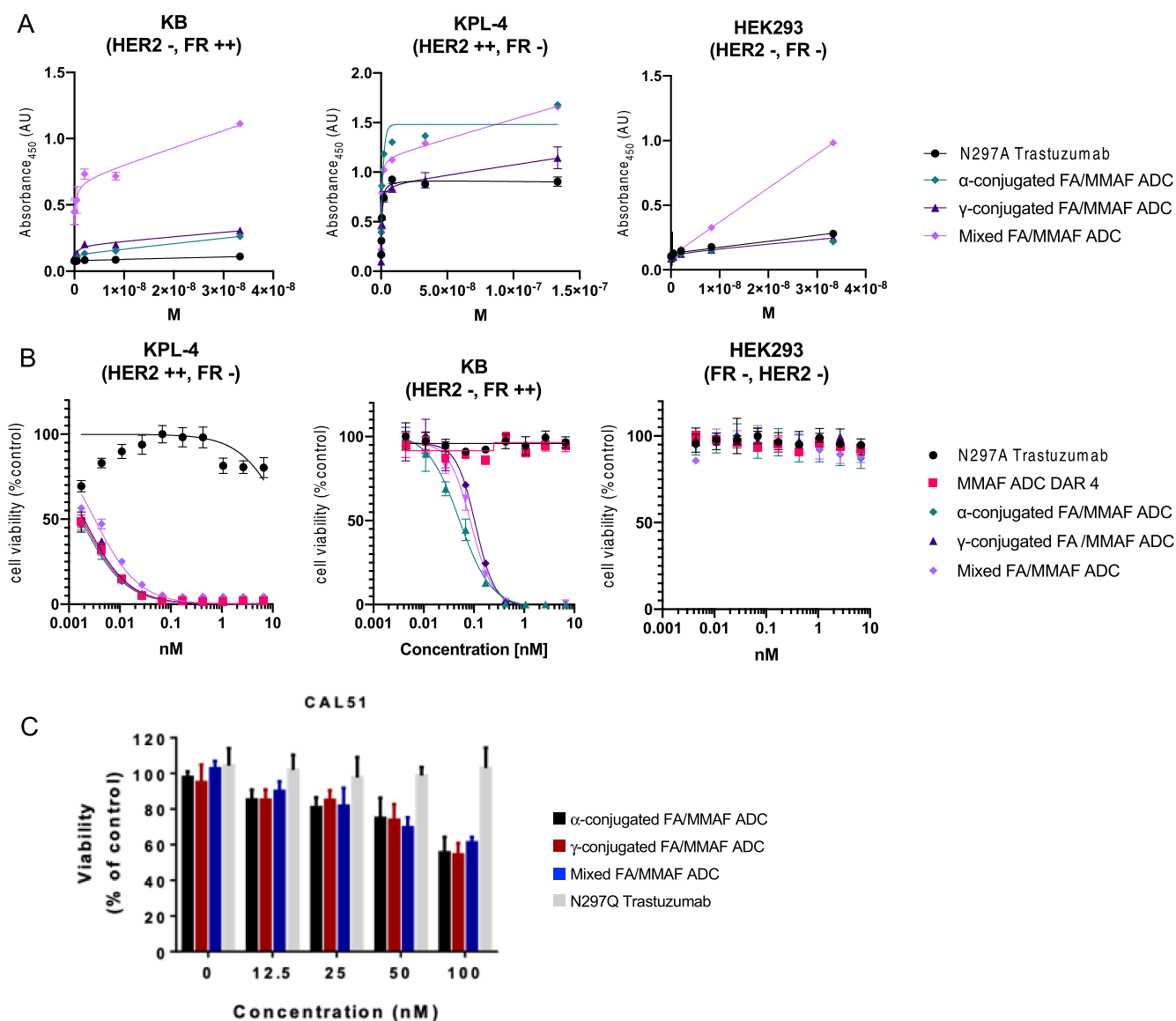


**Figure 4.** FR/HER2 binding assays and in vitro cytotoxicity assay. A, FR/HER2 binding assays. Saturation-binding curves obtained by cell-based ELISA. All assays were performed in triplicate and error bars represent s.e.m. B, In vitro cytotoxicity of ADCs. Cytotoxicity of unconjugated N297A anti-HER2 mAb (black), MMAF DAR4 single-drug ADC (magenta square),  $\alpha$ -conjugated FA FR/HER2 bispecific ADC (green diamond),  $\gamma$ -conjugated FA FR/HER2 bispecific ADC (dark purple triangle), and mixed-FA FR/HER2 bispecific ADC (light purple diamond) in KPL-4 (left panel), KB (middle panel), and HEK293 (right panel). C, Clonogenicity assay for the  $\alpha$ -,  $\gamma$ -, and mixed-FA bispecific ADCs in CAL51 cells. N297Q trastuzumab was used as a control.

module interact with FR. Indeed, Tagawa et al.<sup>14</sup> suggested that a long PEG linker ( $n = 12$ ) could increase binding affinity of a FA-modified mAb for FR by suppressing steric repulsion between the conjugate and FR. Our results also indicate that the FA derivatization position ( $\alpha$  or  $\gamma$ ) does not significantly affect the binding affinity for FR-positive KB cells, which is consistent with previous observation.<sup>24,26</sup> We also confirmed that all ADCs retained high binding affinity for FR negative, HER2-positive KPL-4 ( $K_D$ : 0.29–0.50 nM) but not for HEK293 (FR-negative, HER2-negative). These results demonstrate that our molecular design provides anti-HER2 ADCs with dual-targeting functionality and specificity for FR in addition to HER2.

#### 2.4. Assessment of cell killing potency in vitro.

We next evaluated these bispecific FR/HER2 ADCs for in vitro cytotoxicity in KB, KPL-4, and HEK293 cells (Figure 4B). These ADCs exhibited great potency in both KB (FR-positive, HER2-negative) and KPL-4 (FR-negative, HER2-positive) cells, while the anti-HER2 monospecific MMAF ADC showed cytotoxicity only in the KPL-4 cells. Despite the difference in binding affinity for each receptor, all bispecific FR/HER2 ADCs showed comparable cell killing potencies in KB cells ( $EC_{50}$  values: 52–107 pM). The range of the  $EC_{50}$  values in KPL-4 cells was 1.7–3.2 pM (Figure 4B). No significant toxicity was observed in HEK293 cells for either ADC (Figure 4B). To further explore the cell killing potency of the bispecific FR/HER2 ADCs, we evaluated in vitro cytotoxicity in CAL51, a triple-negative breast cancer cell line expressing FR.<sup>27</sup> Triple-negative breast cancer is a notoriously refractory breast cancer type due to lack of expression of estrogen receptor, progesterone receptor, and HER2, which are targetable with currently approved therapeutic agents. The bispecific FR/HER2 ADCs exhibited a growth inhibition effect at high concentrations (>50 nM, Figure 4C). Taken

together, these results indicate that conjugation of FA with a given anti-HER2 ADC could help treat FR positive tumors regardless of the HER2 expression level.

#### 2.5. Design and construction of integrin/HER2 bispecific ADCs

Encouraged by the results described above, we sought to test the applicability of our branched linker technologies for another format: RGD peptide-appended ADCs. Studies have shown that bivalency and increased local concentration of cyclic RGD peptides can lead to high binding affinity for integrin  $\alpha\beta_3$ .<sup>21</sup> Therefore, we designed a RGD-dimer module consisting of DBCO as a click reaction handle, PEG4 spacers, glutamate as a branching point, and cyclic arginine-glycine-aspartic acid-D-phenylalanine-lysine (RGDfK) peptides (Figure 1A). Anti-HER2 mAb-tri-arm linker conjugates were prepared as described above (Section 2.1). The anti-HER2 mAb-linker conjugates underwent consecutive methyltetrazine-TCO and azide-DBCO cycloadditions in one pot with TCO-MMAF and DBCO-RGD dimer modules. These cycloadditions afforded homogeneous bispecific ADCs with L/DAR values of  $8 + 2$  and  $16 + 4$  (RGD/MMAF) in a quantitative and selective manner (third and fourth panels, Figure 5A and B). Of note, our conjugation afforded the highly loaded RGD/MMAF  $16 + 4$  conjugate as the sole product without yielding any undesired byproducts. These results underscore the design flexibility and preciseness of our branched linker technologies.

#### 2.6. Characterization of integrin/HER2 bispecific ADCs

We then assessed the relative hydrophobicity, in vitro stability, and payload release rates of the integrin/HER2 bispecific ADCs. HIC analysis showed that both conjugates have comparable hydrophobicity

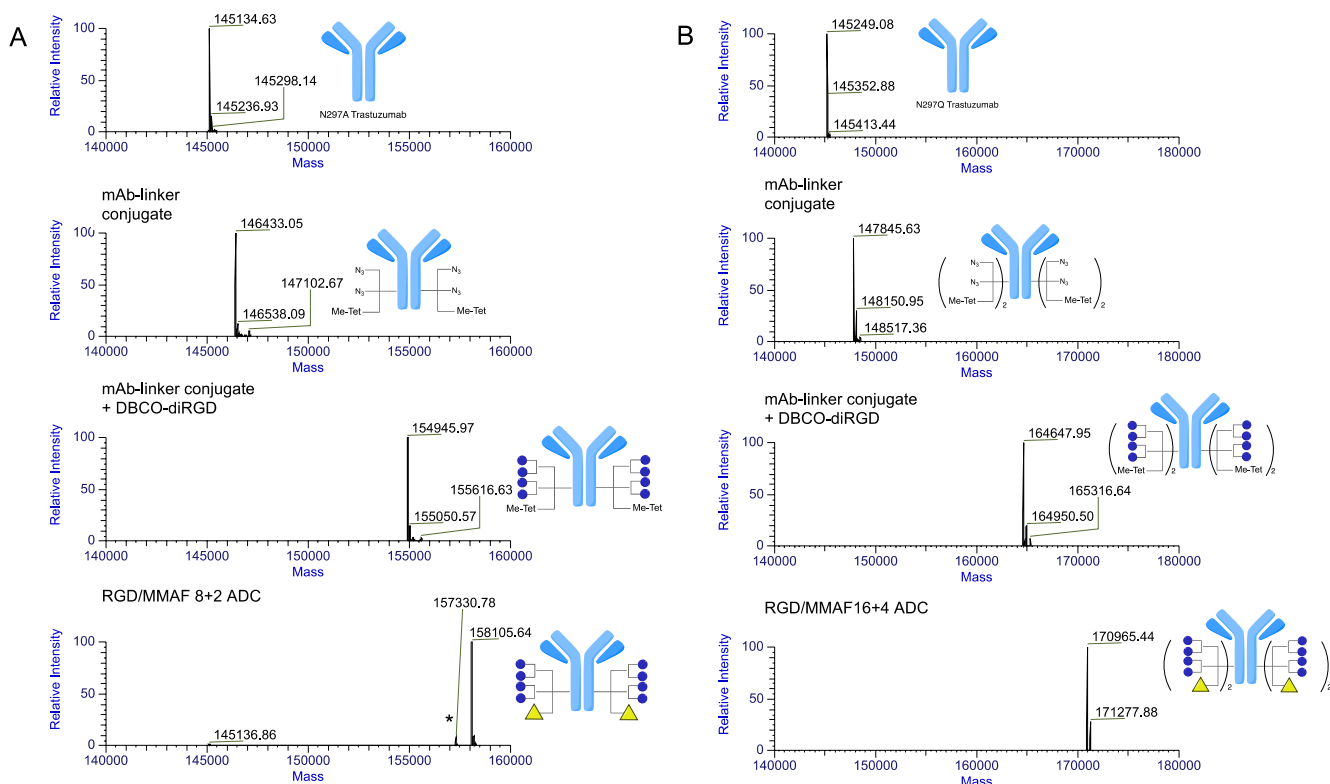


**Figure 5.** Deconvoluted ESI-mass spectra. A, First panel: intact N297A anti-HER2 mAb (trastuzumab mutant). Second panel: antibody-branched linker conjugate. Third panel: intermediate after conjugation with DBCO-diRGD modules (blue circle). Fourth panel: highly homogeneous integrin/HER bispecific ADCs with a L/DAR of  $8 + 2$  (RGD/MMAF depicted as a yellow triangle). Asterisk (\*) indicates fragment ions detected in ESI-MS analysis. B, First panel: intact N297Q anti-HER2 mAb (trastuzumab mutant). Second panel: antibody-branched linker conjugate. Third panel: intermediate after conjugation with DBCO-diRGD modules. Fourth panel: highly homogeneous integrin/HER bispecific ADCs with a L/DAR of  $16 + 4$  (RGD/MMAF).

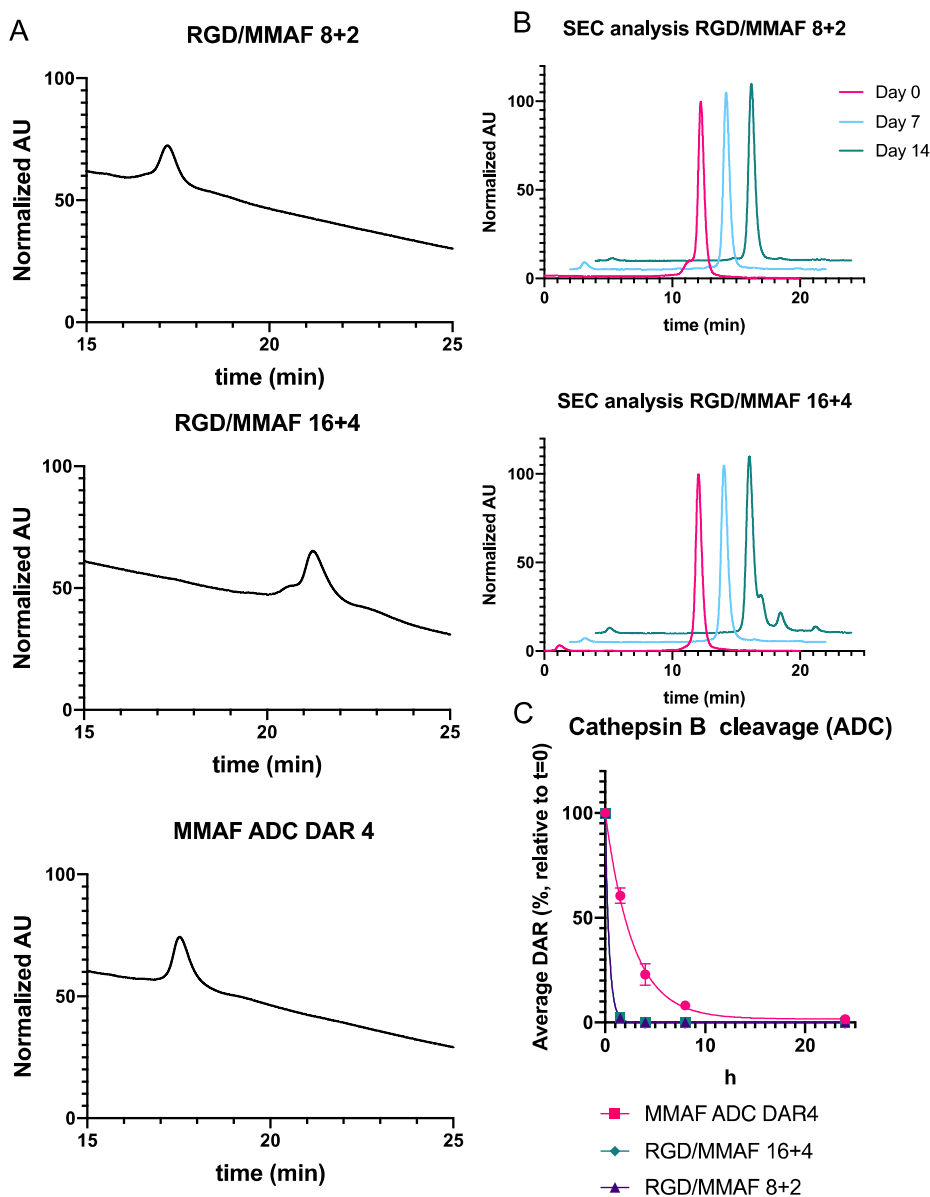


**Figure 6.** Characterization of integrin/HER2 bispecific ADCs. A, Hydrophobic interaction chromatography (HIC) analysis of ADCs under physiological conditions (phosphate buffer, pH 7.4). B, Overlay traces of size exclusion chromatography (SEC) after incubating each conjugate in PBS (pH 7.4) at 37 °C for 0–14 days. No significant aggregation was detected in either case. C, Human cathepsin B mediated cleavage of ADCs at 37 °C. The degree of loss of payload in each ADC was determined by LCMS. All assays were performed more than twice in technical duplicate. Error bars represent s.e.m. (n = 2).

(Figure 6A). SEC analysis revealed that the 8 + 2 bispecific ADC remained intact after incubation in PBS (pH 7.4) at 37 °C for 14 days (Figure 6B). However, the 16 + 4 ADC showed a certain degree of degradation at day 14. Given that circulation half-lives of ADCs equipped with the GluValCit linker system are usually 12–16 days,<sup>25</sup> the compromised stability could affect in vivo performance of this conjugate. Investigation into the cause of the decreased thermal stability, structural modification and further improvement in the stability are underway in our laboratory. In the subsequent cathepsin B assay, payloads were completely released from both conjugates within 4 h, which is in line with our findings with the FR/HER2 bispecific ADCs.

### 2.7. Binding of bispecific integrin/HER2 ADCs to integrin- and/or HER2-positive cell lines

Subsequently, we tested the 16 + 4 and 8 + 2 integrin/HER2 ADCs for binding affinity for integrin and HER2 by ELISA. We used the human cell lines U-87ΔEGFR (integrin  $\alpha\beta 3$ -positive, HER2-negative), KPL-4 (integrin  $\alpha\beta 3$ -negative, HER2-positive), and HEK293 (integrin  $\alpha\beta 3$ - and HER2-negative) (Figure 7A). Both ADCs showed similar binding profiles in integrin  $\alpha\beta 3$  positive U-87ΔEGFR cells despite the difference

in the cyclic RGD loading level, suggesting eight cyclic RGD molecules are sufficient to achieve efficient binding to integrin  $\alpha\beta 3$ . As expected, the intact anti-HER2 mAb did not bind to U-87ΔEGFR cells. We also confirmed that all ADCs retained high binding affinity for KPL-4 ( $K_D$ : 0.41–1.08 nM) but not for HEK293. Collectively, these results suggest that the integrin/HER2 bispecific ADCs have the potential to target tumors with heterogeneous integrin/HER2 expression.

### 2.8. Assessment of cell killing potency in vitro

Finally, we evaluated the RGD dimer-conjugated 16 + 4 and 8 + 2 integrin/HER2 bispecific ADCs for in vitro cytotoxicity in U-87ΔEGFR, KPL-4, and HEK293 cells (Figure 7B). The integrin/HER2 bispecific ADCs exhibited dose-dependent growth inhibition in integrin  $\alpha\beta 3$ -positive, HER2-negative U-87ΔEGFR cells. In particular, the 16 + 4 ADC was more potent ( $EC_{50}$ : 3.58 nM) than the 8 + 2 ADC ( $EC_{50}$ : 36.8 nM). While target-specific cytotoxicity was observed, the  $EC_{50}$  values are higher than those commonly observed for ADCs (<1 nM). These results suggest that further improvement in the design of the RGD dimer-module and conjugates would be required to effectively treat integrin-positive, HER2-negative tumor cells. These ADCs retained high

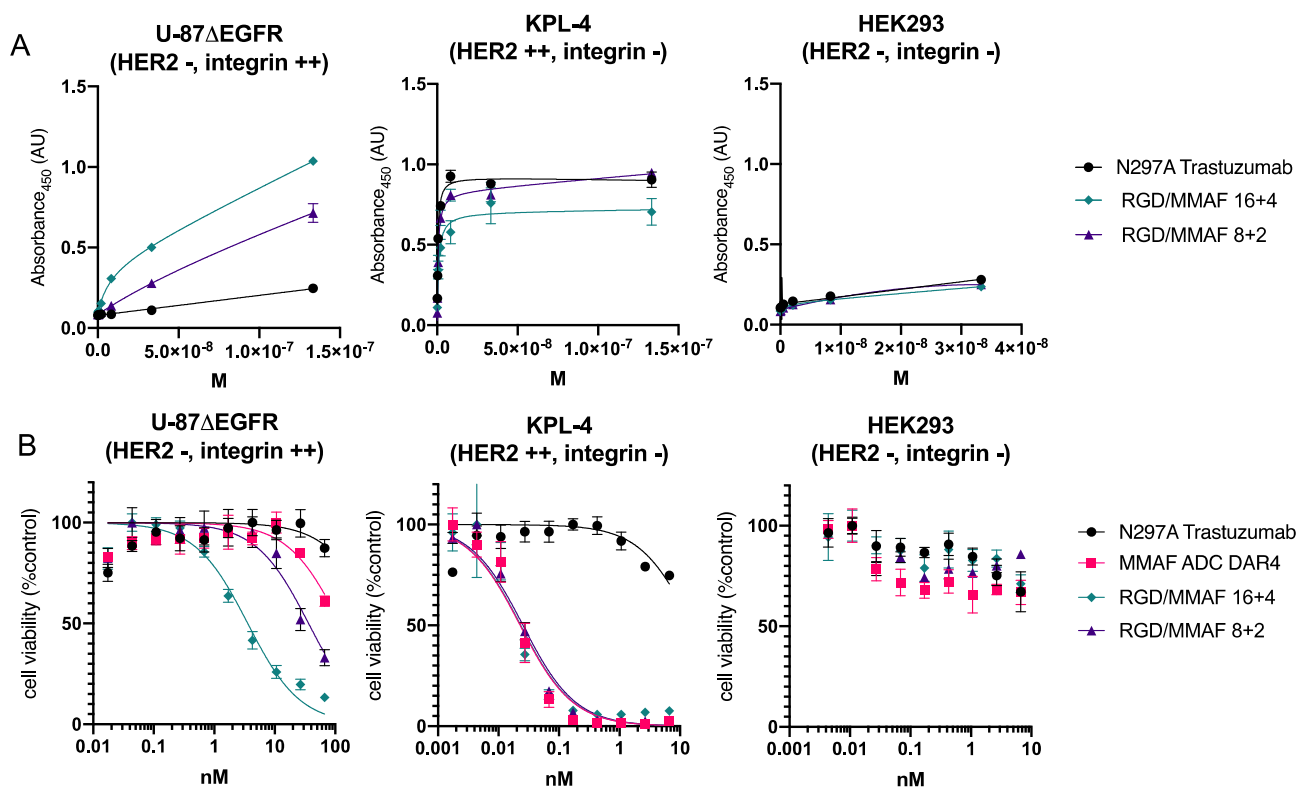


**Figure 7.** Integrin/HER2 binding assays and in vitro cytotoxicity assay. A, Integrin/HER2 binding assays. Saturation-binding curves obtained by cell-based ELISA. All assays were performed in triplicate and error bars represent s.e.m. B, In vitro cytotoxicity of ADCs. Cytotoxicity of unconjugated N297A anti-HER2 mAb (black), MMAF DAR4 single-drug ADC (magenta square), 16 + 4 integrin/HER2 bispecific ADC (green diamond), 8 + 2 integrin/HER2 bispecific ADC (dark purple triangle) in U-87ΔEGFR (left panel), KPL-4 (middle panel), and HEK293 (right panel).

cytotoxicity to the integrin negative, HER2-positive KPL-4 cells. The EC<sub>50</sub> values (19 pM and 29 pM for the 16 + 4 and 8 + 2 ADCs, respectively) were comparable to that of a variant without the RGD module (22 pM) (middle panel, Figure 7B). No significant toxicity was observed in the integrin αvβ3- and HER2-negative HEK293 for either ADC (right panel, Figure 7B). Overall, these results validate our molecular design for the production of small-molecule-based bispecific ADCs.

### 3. Conclusion

This study showed that our branched linker technologies could provide highly homogeneous small molecule-based bispecific ADCs in a precise manner. This methodology enabled flexible and controlled production of bispecific ADCs with L/DAR ranging from 4 + 4 to 16 + 4. Both FR/HER2 and integrin/HER2 bispecific ADCs showed binding and cytotoxicity only in the cells expressing at least either antigen. These results suggest that small molecule-based bispecific ADCs could potentially treat tumors with heterogeneous antigen expression. We expect that, along with further refinement of physicochemical properties and cancer targeting ligand-based potency, future in vivo testing for pharmacokinetics, tumor targeting, and safety profiles will underscore the clinical potential of our bispecific ADC design.

## 4. Materials and methods

### 4.1. Compounds

Synthesis details and characterization data of all new compounds in this study are described in the [Supplementary Data](#).

### 4.2. MTGase-mediated antibody-linker conjugation

Anti-HER2 IgG1 with a N297Q mutation (250 μL in PBS, 10.0 mg mL<sup>-1</sup>, 2.5 mg antibody) was incubated with di-arm linker (13.3 μL of 100 mM stock in DMSO, 80 equiv.) and Activa TI® (64.6 μL of 40% solution in PBS, Ajinomoto, purchased from Modernist Pantry) at room temperature for 16–20 h. The reaction was monitored using a Thermo Vanquish UHPLC coupled with a Q Exactive™ Hybrid Quadrupole-Orbitrap™ Mass Spectrometer equipped with a C18 reverse-phase column (MabPac™ RP column, 4 μm, 2.1 × 50 mm, Thermo Scientific). Elution conditions were as follows: mobile phase A = water (0.1% formic acid); mobile phase B = acetonitrile (0.1% formic acid); gradient over 4 min from A:B = 75:25 to 1:99; flow rate = 0.4 mL min<sup>-1</sup>. The crude products were purified by SEC (Superdex 200 increase 10/300 GL, GE Healthcare, solvent: PBS, flow rate = 0.6 mL min<sup>-1</sup>) to afford an mAb-linker conjugate (2.1 mg, 84% yield determined by bicinchoninic acid assay).

### 4.3. One-pot, double click reactions for payload installation

TCO-peg4-α-conjugated folic acid (14.9 μL of 5 mM stock solution in DMSO, 4.0 equivalent per tetrazine group) was added to a solution of the mAb-linker conjugate in PBS (175 μL, 4.0 mg mL<sup>-1</sup>), and the mixture was incubated at room temperature for 2 h. The reaction was monitored using a Thermo Q Exactive system equipped with a MabPac RP column. DBCO-GluValCit-MMAF (6.0 μL of 5 mM stock solution in DMSO, 1.5 equivalent per azide group) were added to the mixture and incubated at room temperature for 2 h. The crude products were then purified by SEC to afford α-FA-conjugated bispecific FR/HER2 ADC (>95% yield determined by bicinchoninic acid assay). Analysis and purification conditions were the same as described above (see the previous section). Average L/DAR values were determined based on UV peak areas. γ-FA-

and mix-FA-conjugated bispecific FR/HER2 ADCs and bispecific integrin/HER2 ADCs were prepared in the same manner. Purified ADCs were formulated in PBS and stored at 4 °C.

#### 4.4. HIC analysis

Each ADC (1 mg mL<sup>-1</sup>, 10 µL in PBS) was analyzed using an Agilent 1100 HPLC system equipped with a MAbPac HIC-Butyl column (4.6 × 100 mm, 5 µm, Thermo Scientific). Elution conditions were as follows: mobile phase A = 50 mM sodium phosphate containing ammonium sulfate (1.5 M) and 5% isopropanol (pH 7.4); mobile phase B = 50 mM sodium phosphate containing 20% isopropanol (pH 7.4); gradient over 30 min from A:B = 99:1 to 1:99; flow rate = 0.5 mL min<sup>-1</sup>.

#### 4.5. Long-term stability test

Each ADC (1 mg mL<sup>-1</sup>, 100 µL) in PBS was incubated at 37 °C. Aliquots (10 µL) were taken at each time point (7 and 14 days) and immediately stored at -80 °C until use. Samples were analyzed using an Agilent 1100 HPLC system equipped with a MAbPac SEC analytical column (4.0 × 300 mm, 5 µm, Thermo Scientific). Elution conditions were as follows: flow rate = 0.2 mL min<sup>-1</sup>; solvent = PBS.

#### 4.6. Human cathepsin cleavage assay

Each ADC (1 mg mL<sup>-1</sup>) in 30 µL of MES buffer (10 mM MES-Na, 40 µM DTT, pH 5.0) was incubated at 37 °C for 10 min. To the solution was added pre-warmed human cathepsin B (20 ng µL<sup>-1</sup>, EMD Millipore) in 30 µL MES buffer, followed by incubation at 37 °C. Aliquots (20 µL) were collected at each time point (4, 8, and 24 h) and treated with EDTA-free protease inhibitor cocktails (0.5 µL of 100X solution, Thermo Scientific). All samples were analyzed using a Thermo Vanquish UHPLC coupled with a Q Exactive™ Hybrid Quadrupole-Orbitrap™ Mass Spectrometer equipped with a C18 reverse-phase column (MabPac™ RP column, 4 µm, 2.1 × 50 mm, Thermo Scientific). Elution conditions were as follows: mobile phase A = water (0.1% formic acid); mobile phase B = acetonitrile (0.1% formic acid); gradient over 4 min from A:B = 75:25 to 1:99; flow rate = 0.4 mL min<sup>-1</sup>. Average L/DAR values were determined based on mass intensities.

#### 4.7. Cell culture

KB (ATCC) was cultured in folic acid-free RPMI1640 (Corning) supplemented with 10% EquaFETAL® (Atlas Biologicals), GlutaMAX® (2 mM, Gibco), sodium pyruvate (1 mM, Corning), and penicillin-streptomycin (penicillin: 100 units mL<sup>-1</sup>; streptomycin: 100 µg mL<sup>-1</sup>, Gibco). CAL51 cells (Leibniz Institute DSMZ) was cultured under the same conditions except that the culture medium contained folic acid. KPL-4 (provided by Dr. Junichi Kurebayashi at Kawasaki Medical School), U-87ΔEGFR (provided by Dr. Balveen Kaur at the University of Texas Health Science Center at Houston), and HEK293 (ATCC) were cultured in DMEM (Corning) supplemented with 10% EquaFETAL®, GlutaMAX® (2 mM), and penicillin-streptomycin (penicillin: 100 units mL<sup>-1</sup>; streptomycin: 100 µg mL<sup>-1</sup>). All cells were cultured at 37 °C under 5% CO<sub>2</sub> and passaged before becoming fully confluent up to 10 passages. All cell lines were periodically tested for mycoplasma contamination.

#### 4.8. Cell-based ELISA

Cells (KB, U-87ΔEGFR, KPL-4 or HEK293) were seeded in a culture-treated 96-well clear plate (10,000 cells per well in 100 µL culture medium) and incubated at 37 °C under 5% CO<sub>2</sub> for 24 h. Paraformaldehyde (8%, 100 µL) was added to each well and incubated for 15 min at room temperature. The medium was aspirated and the cells were washed three times with 100 µL of PBS. Cells were treated with 100 µL of

blocking buffer (0.2% BSA in PBS) with agitation at room temperature for 2 h. After the blocking buffer was discarded, serially diluted ADC samples (in 100 µL PBS containing 0.1% BSA) were added and the plate was incubated overnight at 4 °C with agitation. The buffer was discarded and the cells were washed three times with 100 µL of PBS containing 0.25% Tween 20. Cells were then incubated with 100 µL of donkey anti-human IgG-HRP conjugate (diluted 1:10,000 in PBS containing 0.1% BSA, Jackson ImmunoResearch) at room temperature for 1 h. The plate was washed three times with PBS containing 0.25% Tween 20, and 100 µL of TMB substrate (0.1 mg mL<sup>-1</sup>) in phosphate-citrate buffer/30% H<sub>2</sub>O<sub>2</sub> (1:0.0003 vol to volume, pH 5) was added. After color was developed for 10–30 min, 25 µL of 3 N-HCl was added to each well and then the absorbance at 450 nm was recorded using a plate reader (BioTek Synergy HTX). Concentrations were calculated based on a standard curve. K<sub>D</sub> values were then calculated using Graph Pad Prism 8 software. All assays were performed in triplicate.

#### 4.9. Cell viability assay

Cells (KB, U-87ΔEGFR, KPL-4 or HEK293) were seeded in a culture-treated 96-well clear plate (5,000 cells per well in 50 µL culture medium) and incubated at 37 °C under 5% CO<sub>2</sub> for 24 h. Serially diluted samples (50 µL) were added to each well and the plate was incubated at 37 °C for 72 h. After the old medium was replaced with 80 µL fresh medium, 20 µL of a culture medium containing WST-8 (1.5 mg mL<sup>-1</sup>, Cayman chemical) and 1-methoxy-5-methylphenazinium methylsulfate (1-methoxy PMS, 100 µM, Cayman Chemical) was added to each well, and the plate was incubated at 37 °C for 2 h. After gently agitating the plate, the absorbance at 460 nm was recorded using a plate reader (BioTek Synergy HTX). EC<sub>50</sub> values were calculated using Graph Pad Prism 9 software. All assays were performed in quadruplicate.

#### 4.10. Clonogenicity assay

Sulforhodamine B (SRB) colorimetric assay<sup>28</sup> was performed to evaluate clonogenicity after treatment with our ADCs. CAL51 cells were plated into 24-well plates (2,000 cells per well) and incubated overnight. The cell culture medium was removed and the cells were washed with a fresh folate-free culture medium. The cells were treated with each ADC in a folate-free medium (60 µL) and incubated for 3 h. Subsequently, 190 µL of a folate-containing complete medium was added and the cells were incubated for 5 days. Subsequently, cells were fixed with 5% trichloroacetic acid and then stained with 0.03% of sulforhodamine B solution (Sigma) at room temperature for 30 min. The stained cells were imaged using a GelCount system (Oxford Optronix) and then dissolved in Tris buffer (10 mM). Optical density was determined fluorometrically using a VICTOR X3 plate reader (Ex: 488 nm, Em: 585 nm).

#### Declaration of Competing Interest

The authors declare the following financial interests/personal relationships which may be considered as potential competing interests: Y. A., N.Z., Z.A., and K.T. are named inventors on a patent application relating to the work filed by the Board of Regents of the University of Texas System (PCT/US2018/034363; US-2020-0115326-A1; EU18804968.8-1109/3630189). The remaining authors declare no competing interests.

#### Acknowledgements

We gratefully acknowledge Prof. Junichi Kurebayashi (Kawasaki Medical School) and Prof. Balveen Kaur (The University of Texas Health Science Center at Houston) for kindly providing the cell lines KPL-4 and U-87ΔEGFR. This work was supported by the Department of Defense Breast Cancer Research Program (W81XWH-18-1-0004 and W81XWH-19-1-0598 to K.T.), the Cancer Prevention and Research Institute of

Texas (RP150551 and RP190561 to Z.A.), the Welch Foundation (AU-0042-20030616 to Z.A.), the University of Texas System (Regents Health Research Scholars Award to K.T.), and the Japan Society for the Promotion of Science (postdoctoral fellowship to A.Y. and Y.A.).

## Appendix A. Supplementary material

Supplementary data to this article can be found online at <https://doi.org/10.1016/j.bmc.2021.116013>.

## References

- Chari RVJ, Miller ML, Widdison WC. Antibody-drug conjugates: an emerging concept in cancer therapy. *Angew Chem Int Ed Engl.* 2014;53(15):3796–3827. <https://doi.org/10.1002/anie.201307628>.
- Perez HL, Cardarelli PM, Deshpande S, et al. Antibody–drug conjugates: current status and future directions. *Drug Discovery Today.* 2014;19(7):869–881. <https://doi.org/10.1016/j.drudis.2013.11.004>.
- Tsuchikama K, An Z. Antibody-drug conjugates: recent advances in conjugation and linker chemistries. *Protein & Cell.* 2016;1–14. <https://doi.org/10.1007/s13238-016-0323-0>.
- McCombs JR, Owen SC. Antibody drug conjugates: design and selection of linker, payload and conjugation chemistry. *AAPS J.* 2015;17(2):339–351. <https://doi.org/10.1208/s12248-014-9710-8>.
- Ocaña A, Amir E, Pandiella A. HER2 heterogeneity and resistance to anti-HER2 antibody-drug conjugates. *Breast Cancer Res.* 2020;22:15. <https://doi.org/10.1186/s13058-020-1252-7>.
- Labrijn AF, Janmaat ML, Reichert JM, Parren PWHI. Bispecific antibodies: a mechanistic review of the pipeline. *Nat Rev Drug Discov.* 2019;18:585–608. <https://doi.org/10.1038/s41573-019-0028-1>.
- DeVay RM, Delaria K, Zhu G, et al. Improved lysosomal trafficking can modulate the potency of antibody drug conjugates. *Bioconjug Chem.* 2017;28(4):1102–1114. <https://doi.org/10.1021/acs.bioconjchem.7b00013>.
- de Goeij BECG, Vink T, Napel ten H, et al. Efficient payload delivery by a bispecific antibody-drug conjugate targeting HER2 and CD63. *Mol Cancer Ther.* 2016;15(11):2688–2697. <https://doi.org/10.1158/1535-7163.MCT-16-0364>.
- Andreev J, Thambi N, Perez Bay AE, et al. Bispecific antibodies and antibody-drug conjugates (ADCs) bridging HER2 and prolactin receptor improve efficacy of HER2 ADCs. *Mol Cancer Ther.* 2017;16(4):681–693. <https://doi.org/10.1158/1535-7163.MCT-16-0658>.
- Sellmann C, Doerner A, Knuehl C, et al. Balancing selectivity and efficacy of bispecific epidermal growth factor receptor (EGFR) × c-MET antibodies and antibody-drug conjugates. *J Biol Chem.* 2016;291(48):25106–25119. <https://doi.org/10.1074/jbc.M116.753491>.
- Vallera DA, Oh S, Chen H, Shu Y, Frankel AE. Bioengineering a unique deimmunized bispecific targeted toxin that simultaneously recognizes human CD22 and CD19 receptors in a mouse model of B-cell metastases. *Mol Cancer Ther.* 2010;9(6):1872–1883. <https://doi.org/10.1158/1535-7163.MCT-10-0203>.
- Bachanova V, Frankel AE, Cao Q, et al. Phase I study of a bispecific ligand-directed toxin targeting CD22 and CD19 (DT2219) for refractory B-cell malignancies. *Clin Cancer Res.* 2015;21(6):1267–1272. <https://doi.org/10.1158/1078-0432.CCR-14-2877>.
- Li H, Lu Y, Piao L, et al. Folate-immunoglobulin G as an anticancer therapeutic antibody. *Bioconjug Chem.* 2010;21(5):961–968. <https://doi.org/10.1021/bc900545h>.
- Tagawa H, Maruyama K, Sasaki K, et al. Induction of ADCC by a folic acid–mAb conjugate prepared by tryptophan-selective reaction toward folate-receptor-positive cancer cells. *RSC Adv.* 2020;10(28):16727–16731. <https://doi.org/10.1039/D0RA03291C>.
- Kranz DM, Patrik TA, Brigle KE, Spinella MJ, Roy EJ. Conjugates of folate and anti-T-cell-receptor antibodies specifically target folate-receptor-positive tumor cells for lysis. *Immunology.* 1995;92:9057–9061.
- Schraa AJ, Kok RJ, Botter SM, et al. RGD-modified anti-CD3 antibodies redirect cytolytic capacity of cytotoxic T lymphocytes toward  $\alpha\beta 3$ -expressing endothelial cells. *Int J Cancer.* 2004;112(2):279–285. <https://doi.org/10.1002/ijc.20413>.
- Panowski S, Bhakta S, Raab H, Polakis P, Junutula JR. Site-specific antibody drug conjugates for cancer therapy. *mAbs.* 2013;6(1):34–45. <https://doi.org/10.4161/mabs.27022>.
- Yamazaki C.M., Yamaguchi A., Anami Y., et al. Antibody-drug conjugates with dual payloads for combating breast tumor heterogeneity and drug resistance. *bioRxiv.* doi: 10.1101/2020.12.18.423326.
- Weitman SD, Lark RH, Coney LR, et al. Distribution of the folate receptor GP38 in normal and malignant cell lines and tissues. *Cancer Res.* 1992;52(12):3396–3401.
- Danhier F, Le Breton A, Pr at V. RGD-based strategies to target  $\alpha(v)\beta(3)$  integrin in cancer therapy and diagnosis. *Mol Pharm.* 2012;9(11):2961–2973. <https://doi.org/10.1021/mp3002733>.
- Liu S. Radiolabeled cyclic RGD peptides as integrin  $\alpha\beta 3$ -targeted radiotracers: maximizing binding affinity via bivalency. *Bioconjug Chem.* 2009;20(12):2199–2213. <https://doi.org/10.1021/bc900167c>.
- Anami Y, Xiong W, Gui X, et al. Enzymatic conjugation using branched linkers for constructing homogeneous antibody–drug conjugates with high potency. *Org Biomol Chem.* 2017;15(26):5635–5642. <https://doi.org/10.1039/C7OB01027C>.
- Anami Y, Deng M, Gui X, et al. LILRB4-targeting antibody-drug conjugates for the treatment of acute myeloid leukemia. *Mol Cancer Ther.* 2020;19(11):2330–2339. <https://doi.org/10.1158/1535-7163.MCT-20-0407>.
- Boss SD, Betzel T, M uller C, et al. Comparative studies of three pairs of  $\alpha$ - and  $\gamma$ -conjugated folic acid derivatives labeled with fluorine-18. *Bioconjug Chem.* 2016;27(1):74–86. <https://doi.org/10.1021/acs.bioconjchem.5b00644>.
- Anami Y, Yamazaki CM, Xiong W, et al. Glutamic acid-valine-citrulline linkers ensure stability and efficacy of antibody-drug conjugates in mice. *Nat Commun.* 2018;9(1):2512. <https://doi.org/10.1038/s41467-018-04982-3>.
- Leamon CP, DePrince RB, Hendren RW. Folate-mediated drug delivery: effect of alternative conjugation chemistry. *J Drug Target.* 2009;7(3):157–169. <https://doi.org/10.3109/10611869909085499>.
- Cheung A, Opzommer JW, Iliava KM, et al. Anti-folate receptor  $\alpha$ -directed antibody therapies restrict the growth of triple negative breast cancer. *Clin Cancer Res.* 2018;24(20):5098–5111. <https://doi.org/10.1158/1078-0432.CCR-18-0652>.
- Vichai V, Kirtikara K. Sulforhodamine B colorimetric assay for cytotoxicity screening. *Nat Protoc.* 2006;1(3):1112–1116. <https://doi.org/10.1038/nprot.2006.179>.